RBRH

Revista Brasileira de Recursos Hídricos
Brazilian Journal of Water Resources
Versão On-line ISSN 2318-0331
RBRH, Porto Alegre, v. 24, e13, 2019
Scientific/Technical Article

https://doi.org/10.1590/2318-0331.241920180030

Evaluation of the energy extraction of a small-scale wave energy converter

Avaliação da extração de energia de um conversor de energia de onda em pequena escala

Carla de Abreu D'Aquino[1], Cesar Cataldo Scharlau[1] and Leonardo Casagrande Dalla Vecchia[2]

[1]Universidade Federal de Santa Catarina, Araranguá, SC, Brasil
[2]Universidade Federal de Santa Catarina, Florianópolis, SC, Brasil
E-mails: carla.daquino@ufsc.br (CAD), cesar.scharlau@ufsc.br (CCS), leonardocasao@hotmail.com (LCV)

Received: March 08, 2018 - Revised: October 29, 2018 - Accepted: January 22, 2019

ABSTRACT

This work aims to focus on proposals that could stimulate the development of small scale integrated devices for the global challenge to provide electric energy from renewable alternative resources without major interventions. It presents an evaluation of a small-scale wave energy extraction system that can be installed in marine near shore structures, such as fishing piers. The system is characterized by a small oscillating-water-column (OWC) converter composed by tubes tied to the pillars of the structure. A mathematical model of the OWC device was developed. The model relies on two main components. The first uses linear wave theory to describe the water level variation inside the tube as a result of a wave passing by. The second considers the air flux converted to mechanical torque using Wells turbine equations. The simulations were carried out for different water depths and wave parameters, to evaluate the ratio between the input and output energy throughout the year. For the case study presented in this paper, the performance would be better as long as the device is placed in a position where the waves are less influenced by the bottom friction, but it still has the necessary increment of the wave height.

Keywords: Wave energy; Oscillating water column device; Simulation; Small-scale; *in situ* wave data.

RESUMO

Este trabalho tem foco em propostas que podem incentivar o desenvolvimento de dispositivos integrados de pequena escala para atender o desafio global de fornecer energia elétrica a partir de fontes alternativas sem maiores intervenções. O artigo apresenta a avaliação de um dispositivo de extração de energia das ondas em pequena escala que pode ser instalado em estruturas marinhas próximas da costa como, por exemplo, uma, uma plataforma de pesca. O dispositivo é caracterizado por um pequeno conversor do tipo coluna de água oscilante composto por tubos fixados aos pilares da estrutura. O modelo matemático desse conversor foi desenvolvido e é baseado em dois componentes principais. O primeiro utiliza a teoria linear de ondas para descrever a variação do nível de água dentro do tubo como resultado da passagem da onda. O segundo considera o fluxo de ar convertido para conjugado mecânico, utilizando as equações de uma turbina *Wells*. Foram realizadas simulações para diferentes profundidades e parâmetros de ondas com objetivo de avaliar a relação entre entrada e a saída de energia ao longo de um ano. Para o estudo de caso apresentado neste artigo, foi observado que o desempenho será melhor quando o dispositivo estiver instalado em locais onde as ondas são menos influenciadas pela fricção com o fundo, mas ainda apresentam o incremento na altura de ondas.

Palavras-chave: Energia das ondas; Dispositivo de coluna de água oscilante; Simulação; Pequena escala; Dados de onda *in situ*.

INTRODUCTION

The development of devices that are able to produce energy using sustainable sources has gathered attention of the research community in the last decades. It is strongly motivated by the appeal to decrease the emission of greenhouse gases and to reduce the impacts of power plants on the environment. Several methods and technologies have been developed based on sustainable sources such as sun, wind and hydro power (rivers and streams). However, there are other sustainable energy sources which might represent interesting alternatives but still require further scientific investigation. Ocean waves may be included in this latter group.

According to Estefen et al. (2006), the energy obtained from ocean waves has the potential to become an important contribution to the Brazilian overall energy production. Brazil has an extensive coastal zone with a wave energy density between 10 and 30 kW/m (CORNETT, 2008; ARINAGA; CHEUNG, 2012). With a 2000 km coastline and an average power density of 20 kW/m, the theoretical potential of the southern and southeastern coast of Brazil can reach 40 GW. The south part of Brazil is characterized by sandy beaches with high energy waves and relatively strong winds. These features represent favorable conditions for using ocean waves as renewable energy resources.

Despite these favorable conditions, the use of ocean waves as energy resource has had few initiatives in Brazil. The Coordination of Engineering Graduate Program (COPPE) of the Federal University of Rio de Janeiro (UFRJ), in partnership with Tractebel S.A., installed the first experimental wave power plant in Brazil at Port of Pecém, Ceará. The plant started to operate in June 2012 with a capacity of 100 kW. The plant is based on a hyperbaric converter with phase control (COSTA; GARCIA-ROSA; ESTEFEN, 2010).

Regarding the technology used for wave energy conversion, the main devices studied in the world can be divided into: oscillating water column (OWC) (FALCÃO; HENRIQUES, 2016; KO et al., 2017); oscillating bodies (FALCÃO, 2010; LIANG; ZUO, 2017); and overtopping (CONTESTABILE et al., 2017). Each one of them has advantages in specific situations. The OWC consists of a structure partially submerged in the water in which, due to ocean wave action, the water level inside oscillates up and down, with the consequent energy being simultaneously transferred to the air volume inside the tube. On the top of the pipe, a power take off (PTO) system transform the kinetic and mechanical power by means of a *Wells* turbine that rotates the axis of a generator, that will convert it into electric power. *Wells* turbines are generally used because of the turbine's direction of rotation is the same in upward and downward movement of air (Figure 1). More details about OWC converters can be found in the review paper of Delmonte et al. (2016).

According to Veigas et al. (2015), the most common configuration for OWC devices is shoreline and bottom mounted. Installation of wave energy conversion devices usually involves preparations and construction of specific facilities, which require time and costs. Besides, the cost of operation and maintenance is also high and can be related with replacements and emergency maintenance, as shown in Astariz and Iglesias (2015). An alternative approach consists on installing these devices in a previously built structure, such as a fishing pier, which is possible with the device considered in this study. This aspect enables the use of the renewable resource with lower costs and without major interventions in the coastal zone. Other advantages of the integration of the plant structure into a breakwater of harbor protection are also emphasized in Falcão and Henriques (2016), such as the shared construction costs and the easier access for build, operation and maintenance of wave energy device. Another example of wave energy extraction system integrated in a breakwater port can be found in Naty, Viviano and Foti (2016).

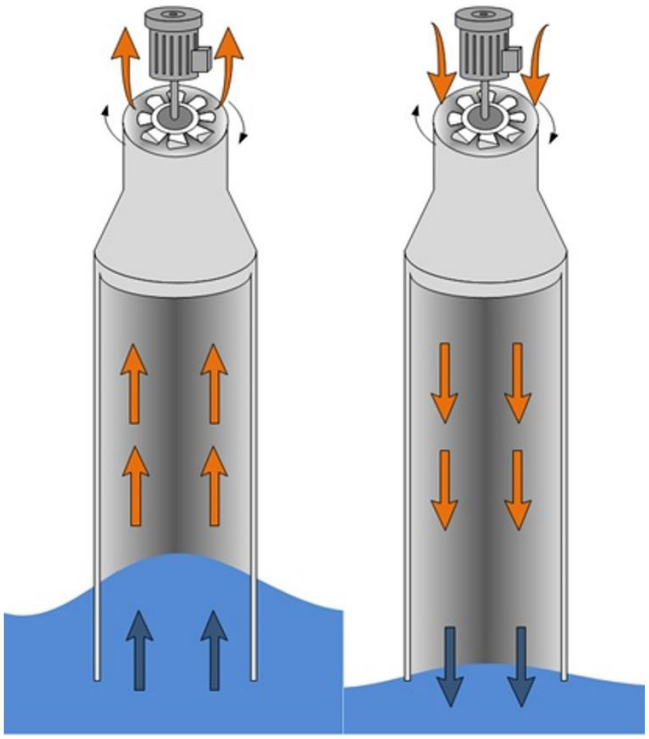

Figure 1. OWC operating principle.

On the other hand, the characteristics of the place of installation, such as water depth, can affect the device performance. For instance, Carballo et al. (2014) showed that the energy production calculated at a 15 m depth location is considerably lower than the one produced at higher depths, except for the case of the OWC technology. This conclusion was based on simulation tests with nine wave energy converters (WEC) using different technologies. The findings by Carballo et al. (2014) also corroborate the choice for OWC device for the case analyzed in the present paper.

The present work proposes an evaluation of the energy extraction of a small-scale wave energy converter installed near shore in a previously built structure. The proposed OWC device is designed for this specific application. A numerical mathematical model of this device is also presented and discussed in this article. The local wave power and other wave characteristics are calculated based on time series wave data collected *in situ* at 17 m depth (intermediate water). This measured wave data is used as input signal for the numerical model. Based on simulation results, it is possible to estimate the available energy resource. In order to demonstrate the application of the proposed evaluation procedures, a case study considering the installation of the OWC device in a

fishing pier at the shore of Tramandaí, Rio Grande do Sul State, Brazil, is presented.

The importance of this work consists on proposing a specific design for the OWC device that takes advantage of a previously built structure, in this case the pillars of the fishing pier, which aims to propose a small-scale solution for the global challenge to provide energy from renewable alternative resources. To the best of authors' knowledge, in Brazilian scientific community there are no other works evaluating OWC devices performance in coastal waters for wave energy conversion. We hope the present paper can promote and inspire new researches in this subject.

Also, the use of measured time series wave data on simulation can represent an improvement on the evaluation of OWC device performance. Most of the previously published results about this subject use mainly equation (i.e LIANG; ZUO, 2017; MISHRA; PURWAR; KISHOR, 2016) or spectrum (i.e. GARCIA-ROSA et al., 2014) to create a random wave that might represent the sea state for a specific location, or simply assume a fixed theoretical wave to test the model.

This paper is organized as follows: the next section presents some general theory on ocean wave energy; section 3 describes the necessary procedures to calculate the wave characteristics based on the data collected *in situ*; section 4 presents the mathematical model of the OWC device considered in this paper. The case study is depicted in Section 5 and simulation results are presented and discussed in Section 6. The paper ends with some concluding remarks.

WAVE ENERGY

The description of the ocean waves is relatively complex since they are the result of various interactions and overlays. In this study, we consider surface gravity waves that are generated by wind. When the waves reach a certain size, the wind may exert a more intense action in their face, causing further growth (DEAN; DALRYMPLE, 1991).

The ocean surface can be interpreted as the sum of several sinusoidal components of different amplitudes, periods and directions with random phases. Consider a progressive wave with water surface displacement (η) given by:

$$\eta(t, x) = a\sin(\omega t - kx) \tag{1}$$

where t is time; x is distance; a is the wave amplitude, which equals half the wave height (H); $\omega = 2\pi / T$ is the wave frequency; T is the wave period; $k = 2\pi / L$ is the wave number; and L is the wave length.

In deep water, ocean waves can travel many kilometers without losing energy. As waves approach the shore, they interact with the seabed and the energy density may decrease due to bottom friction. Also, in the transition between deep, intermediate and shallow water, the wave loses speed, the length decreases and the height increases more and more (shoaling) until the wave becomes unstable and breaking occurs. Since the wave energy is a function of the square of the height, this shape modification plays an important role in estimating the potential of wave energy in shallow water near the shore.

The total energy contained in a wave (E_T) can be determined by the sum of the kinetic energy (E_k), which results for the movement of the water particles through the fluid, and the potential energy (E_p), that results of the displacement of the free surface wave.

For gravity waves, E_T is described by:

$$E_T = E_k + E_p = \frac{1}{2}\rho_{sea} g a^2 \tag{2}$$

where ρ_{sea} is the density of sea water and g is the gravity acceleration.

The wave power flux P_{wave} can be obtained by:

$$P_{wave} = E_T C_g \tag{3}$$

where C_g is the speed at which the energy is transmitted. This velocity is called the group velocity. According to Dean and Dalrymple (1991), for deep waters the energy is transmitted at only half the speed of the wave celerity (C).

In intermediate waters, when $\frac{1}{20} < \frac{h}{L} < \frac{1}{2}$, the group velocity is given by:

$$C_g = CN \tag{4}$$

where

$$C = \sqrt{\frac{gL}{2\pi}\tanh\left(\frac{2\pi h}{L}\right)} \tag{5}$$

$$N = \frac{1}{2}\left(1 + \frac{2kh}{\sinh(2kh)}\right) \tag{6}$$

and h is the local depth.

In shallow waters, the celerity and energy travel at the same speed. Due to the wave changes as it approaches the coast, it is expected a decrease in C due to bottom friction, which can cause an energy loss in the process (DEAN; DALRYMPLE, 1991). Therefore, the waves celerity in the shallow waters $\left(\frac{h}{L} < \frac{1}{20}\right)$ depends only of the local depth. Thus

$$C_g = C \tag{7}$$

where

$$C = \sqrt{gh} \tag{8}$$

At this point, it is important to emphasize that this paper intends to evaluate an application of a wave energy converter installed nearshore (a fishing pier built on the coast), which can be considered shallow water. In addition, the wave data used for the case study was obtained in the intermediate water. Hence, these previous considerations are significant for a more detailed assessment of the energy potential in shallow and intermediate waters and also to evaluate the performance of the device.

WAVE DATA

The time series wave data used in the case study of this paper were collected *in situ* on 17 m deep (h_2)and was extensively discussed in Strauch et al. (2009) and Assis, Beluco and Almeida (2013). Since the device will now be analyzed in shallow water (about 4 m deep, h_1), it is necessary to calculate the wave transformation due to propagation using linear wave theory.

For a straight and long beach with uniform background gradient, as the case studied, the waves tend to propagate perpendicular to the shoreline. Hence, the changes in the wave parameters can be introduced applying the Snell's Law (DEAN; DALRYMPLE, 1991).

$$\frac{C_2}{C_1} = \frac{sin(\alpha_2)}{sin(\alpha_1)} \tag{9}$$

where α is the angle between wave crest and the bottom contour line and C_i is the velocity of a single wave for a given water depth indicated in the sub-index i. It is important to emphasize that the wave period T keeps the same during the transition from deep to shallow waters.

In order to determine the wave height in the depth where the OWC device will be located (H_1), it is necessary to calculate the wave length using the equation below:

$$L_2 = T\sqrt{\left(\frac{g}{k}\right)\tanh(kh)} \tag{10}$$

Based on the values of H_2 (directly measured) and L_2, it is possible to determine the shoaling coefficient (K_s), the α at different depths, and the refraction coefficient (K_r) using the following equations:

$$K_s = \sqrt{\frac{1}{2}\frac{1}{N}\frac{1}{\tanh(kh)}} \tag{11}$$

$$\frac{\sin(\alpha_1)}{\sin(\alpha_2)} = \tanh\left(\frac{2\pi h}{L_2}\right) \tag{12}$$

$$K_r = \sqrt{\frac{\cos(\alpha_2)}{\cos(\alpha_1)}} \tag{13}$$

Lastly, the wave height at the pier depth can be calculated using the following equation (HODGINS; LEBLOND; HUNTLEY, 1985):

$$H_1 = H_2 K_s K_r \tag{14}$$

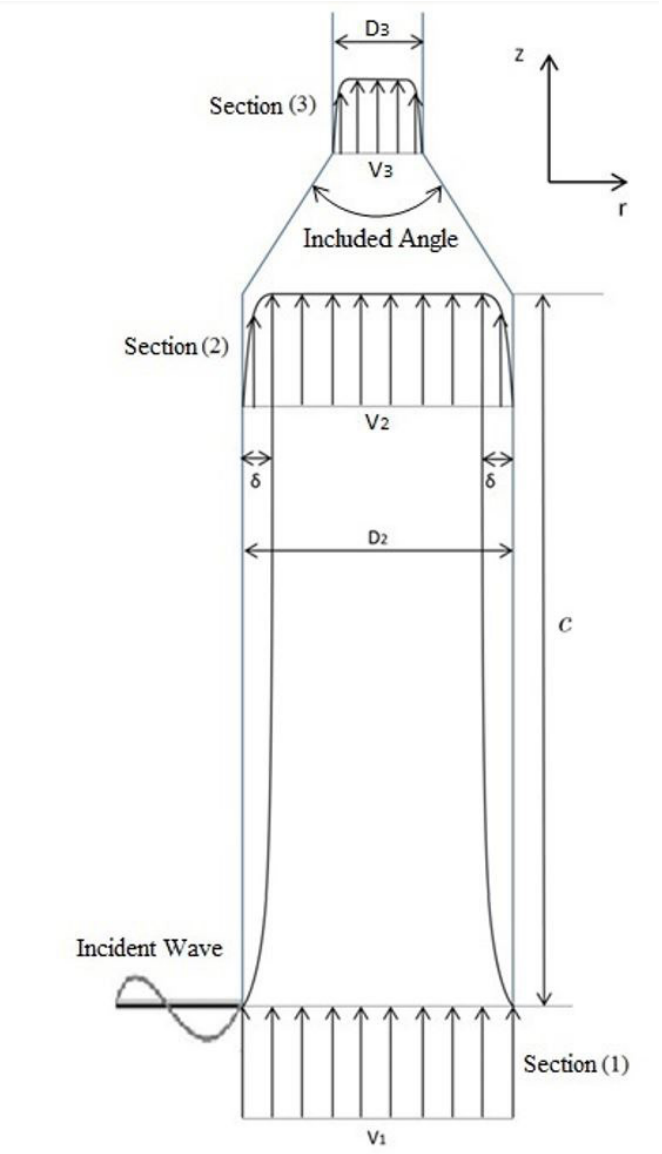

Figure 2. The OWC device considered for energy conversion.

OWC MODELING

This section describes the mathematical model of the OWC device considered in this paper. The device extracts power from the waves using the motion of the water in the chamber to force air through a turbine (BINGHAM et al., 2015). The designed shape of the proposed device (Figure 2), composed by a tube that could be tied to the pillar of several oceanic structures, seems adequate for installation in previously built facilities. A *Wells* turbine is employed for the conversion of kinetic energy into mechanical energy. The present study is only focused on mechanical energy extraction.

The OWC modeling consists in determining the air velocity behavior in section 3 of the device, based on Fluid Mechanics theory and considering the incident wave as input signal. According to Falcão and Henriques (2016), theoretical hydrodynamic modeling of OWCs based on linear water wave theory and hydrodynamic coefficients is still the most frequently adopted approach. The equations of the model describe the physical characteristics of the air flow inside the device and determine the losses of flow velocity due to friction along the tube's walls, the head losses and the contraction. More details about the model are provided in the following subsections.

Incident wave

According to Dean and Dalrymple (1991); Bouali and Larbi (2013) and Vecchia et al. (2015), the incident wave velocity in the OWC device can be described by:

$$V_1 = \frac{H}{2}\frac{gk}{\omega}\frac{\sinh(k(h+z))}{\cosh(kh)}\sin(kx-\omega t) + \frac{3}{16}\frac{H^2\omega k\sinh(2k(h+z))}{\sinh^4(kh)}\sin(2(kx-\omega t)) \tag{15}$$

where z is the variation of the position between the free surface of the water and the seafloor.

For the analysis in this paper, the diffracted and reflected waves' parts can be disregarded, because it is assumed that the tube has a small wall thickness. Thus, it is possible to consider that the vibrations originated by the impact of incident waves do not interfere significantly in the problem.

Air into device

In order to describe the air behavior into the device, the incident wave velocity, modeled in the previous subsection, is used as input signal in the section 1 of the tube in Figure 2.

The water column movement into the device was modeled as a rigid piston with negligible mass. With this consideration, used in Brendmo, Falnes and Lillebekken (1997), it is possible to disregard the speed variation in the r direction. Therefore, the velocity profile in section 1 of Figure 2 can be determined by Equation 15. It was also considered that all the energy of the wave is transmitted to the air above the ocean water surface. Thus, it is possible to consider that the air velocity is equal to the incident wave velocity.

The model of the air into the device is based on two fundamental concepts in fluid mechanics theory. The first one is about the formation of a region where the fluid, in this case the air, is influenced by the tube walls. This influence results in a velocity reduction inside this region, called boundary layer (FOX; MCDONALD; PRITCHARD, 1985). Therefore, the air velocity in section 2 (V_2) depends on the boundary layer thickness and the air velocity in section 1.

First, according to Fox, McDonald and Pritchard (1985), the Reynolds number Re_L based on the tube length is determined by:

$$Re_L = \frac{V_1 L_t}{\nu} \tag{16}$$

where V_1 is the time average velocity of flow in section 1; L_t is the tube length and ν is the kinematic air viscosity. For the case of laminar flows ($Re_L \leq 2300$), the following equations shall be used to calculate V_2:

$$\delta = \frac{5.48 L_t}{\sqrt{Re_L}} \tag{17}$$

$$V_2 = V_1 \left[2\left(\frac{y}{\delta}\right) - \left(\frac{y}{\delta}\right)^2 \right] \tag{18}$$

where δ is the thickness of the boundary layer and y is the distance between the wall and the point analyzed.

On the other hand, for turbulent flows ($Re_L > 2300$), V_2 is determined by:

$$\delta = \frac{0.382 L_t}{Re_L^{1/5}} \tag{19}$$

$$V_2 = V_1 \left(\frac{y}{\delta}\right)^{1/7} \tag{20}$$

The second concept of the fluid mechanics theory, called head loss, is related to the energy loss due to frictional effects in fully developed flow (major losses, h_l) and due to entrances, fittings, area changes, and so on (minor losses, h_{lm}). In the current study, this concept determines the velocity reduction that the tube contraction will cause, given by:

$$h_{lm} = K\left(\frac{\bar{V}_2^2}{2}\right) \tag{21}$$

where $\bar{V}_2$ represents the mean velocity in section 2 of the tube and K is the loss coefficient, described in Table 1 (FOX; MCDONALD; PRITCHARD, 1985).

The area ratio (AR) is given by:

$$AR = \frac{\pi D_3^2}{4}\frac{4}{\pi D_2^2} = \frac{D_3^2}{D_2^2} \tag{22}$$

where D_2 and D_3 represents the diameters of section 2 and 3 of the tube, respectively.

The tube contraction also causes an air acceleration due to the mass conservation law, i.e. all mass that crosses section 2 of the tube will cross section 3. Thus, the air is accelerated respecting the ratio expressed by:

$$\bar{V}_3 = \frac{\bar{V}_2}{AR} \tag{23}$$

where $\bar{V}_3$ is the cross section mean velocity in section 3 of the tube. In Equation 23, it is considered that the density variation of air and the time variation term of the mass conservation law can be disregarded.

When applying Equations 21 and 23 in the Bernoulli equation, it is possible to determine the velocity of the air in section 3 of the tube and, consequently, the kinetic power of the air. More details about this point can be found in Fox, McDonald and Pritchard (1985) and Vecchia et al. (2015).

Turbine

In order to model the conversion of kinetic energy into mechanical energy, a *Wells* turbine is used due to its feature of keeping the same direction of rotation in upward and downward movement of the air flow. Equation 24 shows the relation between the absolute velocity V, the attack angle ϕ and the relative velocity W.

$$W = \frac{V}{\sin(\phi)} \tag{24}$$

Table 1. Loss Coefficients for Gradual Contractions: Round and Rectangular Ducts (FOX; MCDONALD; PRITCHARD, 1985, p. 344).

Included Angle [°]	Area Ratio		
	0.5	**0.25**	**0.10**
10	0.05	0.05	0.05
15-40	0.05	0.04	0.05
50-60	0.06	0.07	0.08
90	0.12	0.17	0.19
120	0.18	0.27	0.29
150	0.24	0.35	0.37
180	0.26	0.41	0.43

Several airfoil profiles can be used on a *Wells* turbine. A comparison between the performance of the airfoil profiles NACA0012, NACA0015, NACA0018, NACA0020 and NACA0021 is presented in Dias et al. (2013) and Mohamed (2011). The references Dias et al. (2013), Raghunathan, Tan and Ombaka (1985) and Webster and Gato (1999) indicate that the NACA0021 profile provides a better performance compared to the other ones.

For the purpose of the performance response of the OWC device, two standard equations for power estimation were applied: mechanical and kinetic. The equation for mechanical power for this turbine can be written as:

$$P_{mec} = \left(\frac{1}{2}\right) n \rho_{air} A V_3^3 \tag{25}$$

where n is the turbine efficiency, ρ_{air} is the air density, A is the swept area of the turbine blades, and V_3 is the absolute velocity of the flow.

The equation for kinetic power is the same that Equation 25, except by the turbine efficiency term that is disregarded:

$$P_{kin} = \left(\frac{1}{2}\right) \rho_{air} A V_3^3 \tag{26}$$

NUMERICAL EXAMPLE

This section presents a numerical example for an OWC device installed in a fishing pier at the coast of Tramandaí beach, south Brazil. Figure 3 shows the location and a photo of the considered fishing pier. The wave data used in this work was acquired at this coast through a directional Datawell Waverider buoy that was deployed in November *2006* at *17* m water depth (STRAUCH et al., 2009) and consists in a time series wave data. The coastal region, extending from Cabo de Santa Marta (Santa Catarina State) to Chuí (Rio Grande do Sul State), is characterized by a rectilinear coastline extensive sandy coastal plains and low altitude (TESSLER; GOYA, 2005). The exposed sandy beaches are dominated by high-energy waves (WRIGHT; SHORT, 1984).

Several authors have already described the wave pattern at the south region of the Brazilian coast, for instance: Siegle and Asp (2007), Alves et al. (2009) and Pianca, Mazzini and Siegle (2010). These studies agreed that the southwest sea waves are dominant at the south Atlantic ocean. This pattern is interrupted when the Atlantic Anticyclonic Gyre dominates the atmospheric surface circulation and the north wave occurs. According to Toldo et al. (2006), the waves pattern of north-northeast are predominant at spring and summer seasons. This pattern can change by the passage of the cold fronts that comes from south-southeast, causing high-energy waves with mean significant wave height of *1.5* m and period between *7* to *9* s. It was also verified in Strauch et al. (2009) that the most energetic events occur in the fall and winter, when the extra-tropical storm generates swells at the south Atlantic ocean. These aspects reinforce the importance of seasonal evaluation of wave data.

In order to evaluate the conversion of ocean waves power in mechanic and kinetic power, simulations were carried out using the waves cases presented in the Table 2, which represent the seasonal means of time series wave data, and also the complete wave data set.

Table 2. Collected wave data used to perform the analysis (STRAUCH et al., 2009).

Season	T (s)	H_{17} (m)
Spring	6.66	1.22
Summer	7.17	1.32
Fall	7.86	1.15
Winter	7.79	1.36
Annual	7.66	1.23

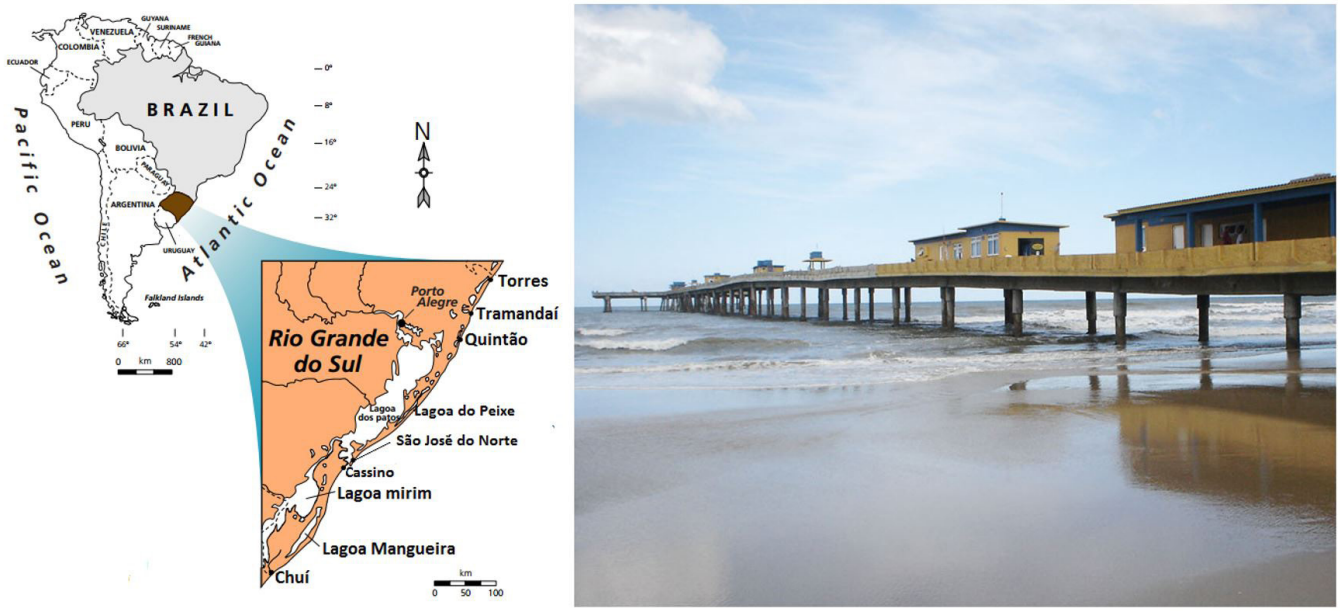

Figure 3. Location and photograph of the fishing pier object of this study in Tramandaí beach, south Brazil.

Tables 3 and 4 present constructive parameters of OWC device and *Wells* turbine, respectively. This design was already tested in Vecchia et al. (2016).

Figure 4 show the simulation diagram used on Matlab/Simulink. The main result will be shown in terms of speed and power.

SIMULATION RESULTS

The annual and seasonal wave characteristic calculated for the two depths are shown in the Table 5, in which the wave direction was considered the same for both depths. The changes in wave direction from deep to shallow water are small due to parallel bathymetry bottom configuration, thus possible differences are neglected. This aspect was also observed in Carballo et al. (2014), which considers the power of wave device as a function of H and T, assuming that it does not depend on the wave direction.

The simulation results for the complete time series data are presented. Figures 5 and 6 show the kinetic, mechanical and wave power for *17* and *4* m of depth, respectively. The gaps in the temporal series represent periods when the wave-meter was in maintenance.

It is found for both depths that, in some cases, the kinetic power is greater than the wave power. In order to better understand these occurrences, it is necessary to investigate the correlation between the wavelength, the wave height, the velocity inside the tube and the power. For this matter, histograms of the measured significant wave height together with simulation results for the power were generated (Figure 7).

In Figures 7a and 7c an increase of the wave power with the wave height can be seen, with less scattered data at *4* m depth due to the bottom friction influence. However, on Figure 7b this relation is not clear. It could also be observed an increase in the kinetic and mechanical power at the points with greater occurrence of high wave heights. For the case of *4* m depth, Figure 7d, an exponential increase of kinetic and mechanical power with the wave height occurs due to the bottom influence before the wave breaking. This figure also shows a scattered increase in the power for the points with greater occurrence of high wave heights.

In order to investigate and better comprehend these results, several correlation curves were generated between the air velocity inside the tube and different wave parameters (Figures 8 and 9). At *17* m deep, there is no correlation between H and that velocity (Figure 8a). However, the curves between L and V (Figure 8b), and T and V (Figure 8c), are well correlated.

These results show that the wave length is important regarding the total energy carried out by waves and transferred to the airflow inside the tube. Both kinetic and mechanical powers are proportional to the cube of air velocity at the last section of the tube, where the mass flux is already most influenced by the tube characteristics and probably less influenced by the wave height. This aspect could be verified by the weak correlation between V and H (Figure 8a).

The obtained results show a dependence of H on the power output smaller than expected, since the energy depends of the square of the wave height. However, Rezanejad et al. (2017) also observed, based on experimental and numerical data, that the influence of the wave height on the performance of the OWC

Table 3. OWC device constructive parameters.

Parameter	Value
Pipe length (L_p)	3 m
Section 2 diameter (D_2)	0.79 m
Section 3 diameter (D_3)	0.25 m
Included angle	60°

Table 4. *Wells* turbine parameters for NACA 0021 profile.

Parameter	Value
Efficiency (n)	0.71
Swept area (A)	0.0471 m²

Table 5. Calculated wave parameters.

Season	α_{17} (°)	L_{17} (m)	H_4 (m)	L_4 (m)
Spring	132.07	64.28	0.99	39.31
Summer	133.54	72.15	1.08	41.66
Fall	124.71	82.38	1.06	46.68
Winter	146.14	81.46	1.09	45.69
Annual	131.56	79.47	1.06	45.88

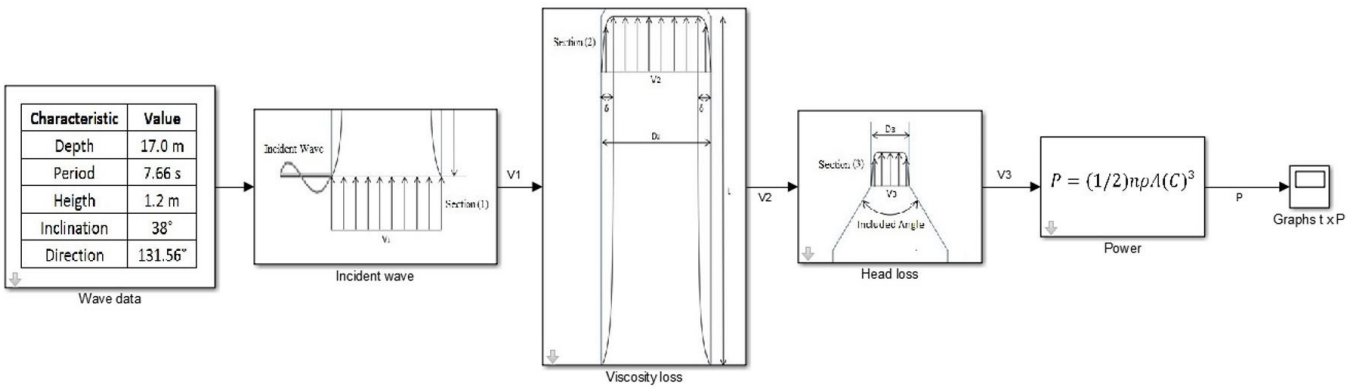

Figure 4. Block diagram for simulink simulations, example for 17 m water depth.

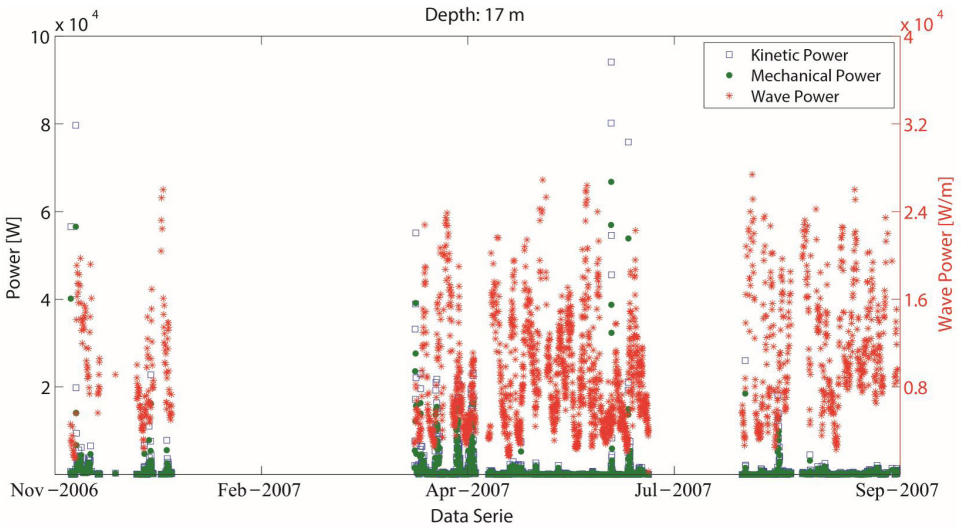

Figure 5. Kinetic, mechanical and wave power for 17 m water depth.

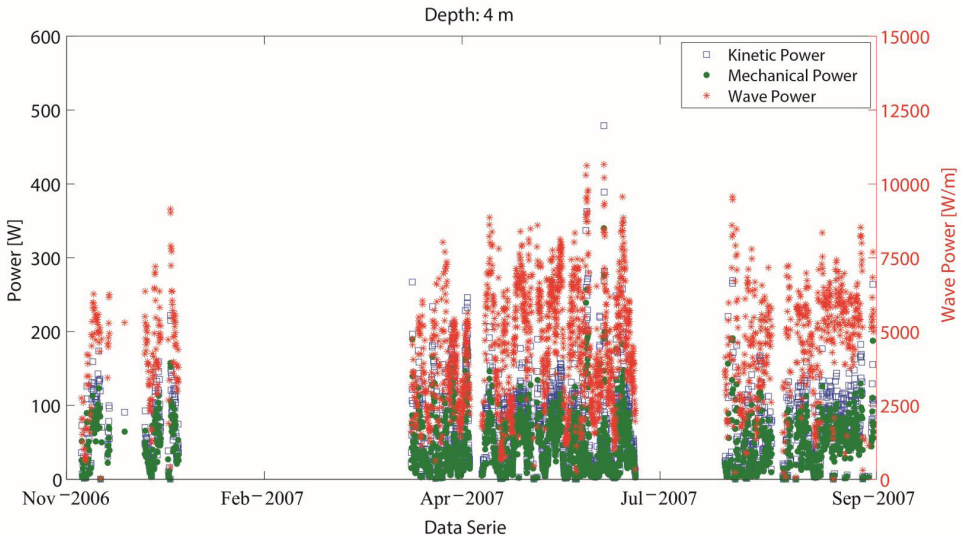

Figure 6. Kinetic, mechanical and wave power for 4 m water depth.

device is of lesser importance as compared to the wave period and turbine damping.

For *4* m depth, the correlation between *H* and *V* shows a more linear relation, while the correlation between *L* and *T* presents a dispersive graphic. The air flow velocity inside the tube results from the mass movement composed both by the wave height and wave length. In this case, the waves are near to the break point. Thus, it presents the minimum wave length and the maximum wave height. Therefore, the velocities inside the tube have a stronger dependence on the wave height, as shown in the correlation coefficient of Figure 9a. Also, the wavelengths for *4* m deep are smaller than the ones in *17* m. This wave length reduction at *4* m deep brings a reduction of *47* % in the annual wave power (P_{wave}) and it represents about *88*% of the reduction of kinetic power inside the tube.

The next round of simulations is intended to compare the response of the system to the differences in the seasonal mean wave high at two different depths: *17* and *4* meters (Tables 6 and 7). The winter shows the highest values of wave power, being higher at *17* m depth. In shallow water, relatively small variations of power (kinetic, mechanical and wave) between the seasons are found. However, by analyzing the kinetic power, it is possible to verify a different response for *4* and *17* m depth. For *17* m water depth, the highest values of wave power are associated with the winter. However, the highest value of mechanical power occurs at spring, which corresponds with the period of time when the smallest wave length is presented (see Table 5).

It is interesting to observe for 4 m depth that the values of mechanical and wave power are near to the annual mean, even with these seasonal variations. The wave power in spring is about *13* % less than the annual mean and the mechanical power is about *7* % less than the annual mean. These results indicate that the OWC device can perform better in the winter and fall. For *17* m depth, a relatively strong correlation of the powers with

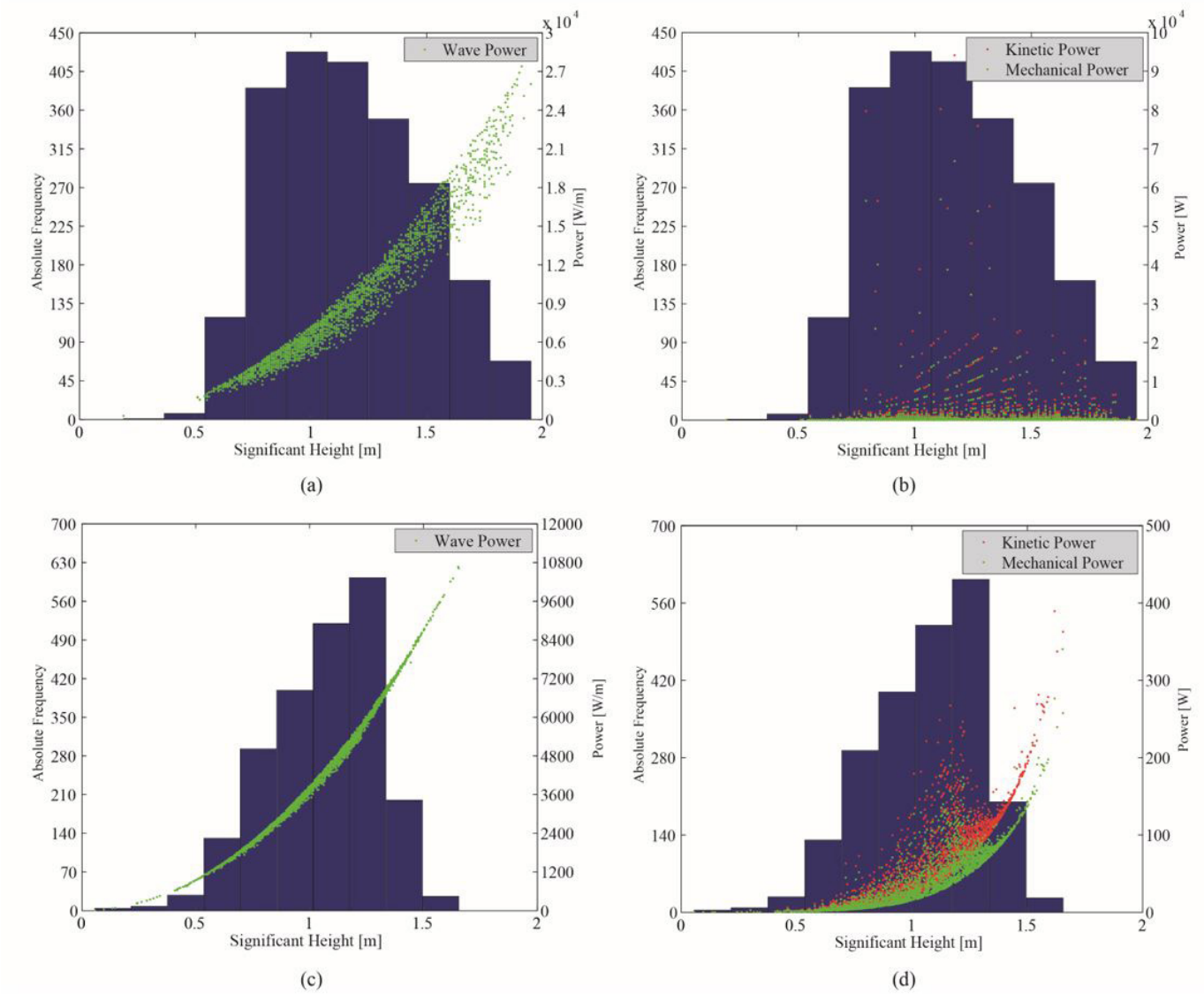

Figure 7. Wave power distribution and kinetic and mechanical power distribution shown for 17 m, (a) and (b), and 4 m, (c) and (d).

Table 6. Powers for the four seasons and the annual mean to 4 m of depth.

	h = 4 m				
	Spring	**Summer**	**Fall**	**Winter**	**Annual**
P_{wave} [W/m]	3878.08	4540.29	4418.37	4637.00	4459.23
P_{kin} [W]	62.03	77.99	66.44	66.45	66.72
P_{mec} [W]	44.04	55.37	47.17	47.18	47.36

Table 7. Powers for the four seasons and the annual mean to 17 m of depth.

	h = 17 m				
	Spring	**Summer**	**Fall**	**Winter**	**Annual**
P_{wave} [W/m]	9152.52	9359.08	8679.15	11008.56	9359.95
P_{kin} [W]	2722.45	1305.67	1279.60	447.34	1117.14
P_{mec} [W]	1932.81	926.96	908.46	317.59	793.12

the seasons is found. Table 7 shows that the wave power in winter is *20.3* % greater than in spring. On the other hand, the mechanical power has the opposite behavior, with a value *508.6* % greater in spring than in winter.

Next, it is evaluated the influence of the depth on the powers. Those values were obtained using Equations 8 until 14 and Equations 3, 25 and 26 for wave, mechanical and kinetic powers, respectively. Figure 10 shows the correlation between the depth and the wave power, that occurs mainly because of the interaction between the wave and the ocean floor. This interaction reduces the wave celerity and, consequently, the wave power. The linear loss of wave power results from the equilibrium between the action of the friction with the bottom and the gain in the wave height due to refraction process. However, the mechanical and kinetic powers present an exponential decay as long as approaches the shallow waters, due to the proportionality of the cube of air velocity (Equations 25 and 26).

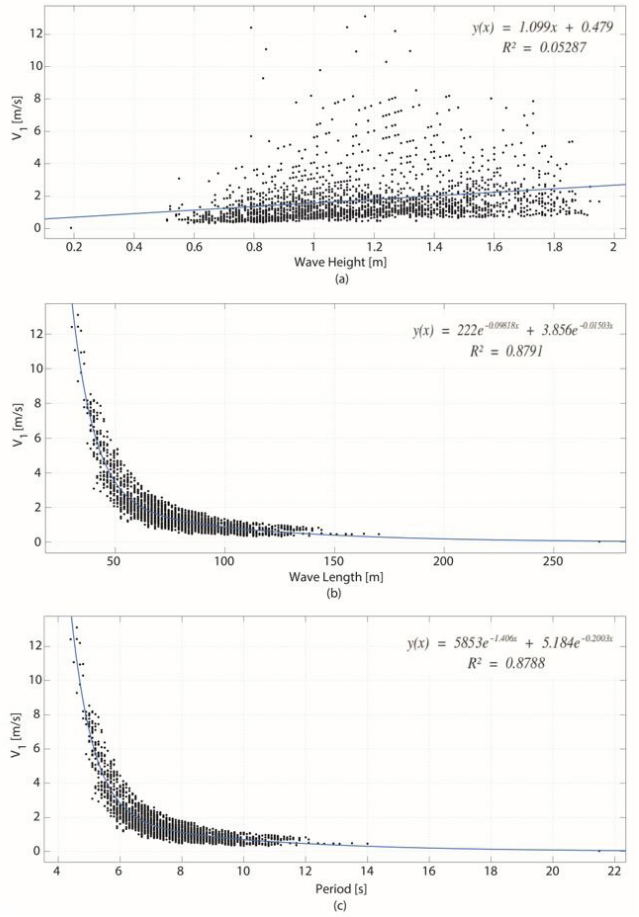

Figure 8. Correlations between air velocity in section 1 and wave height (a), wave length (b), and wave period (c) for the case with 17 m deep.

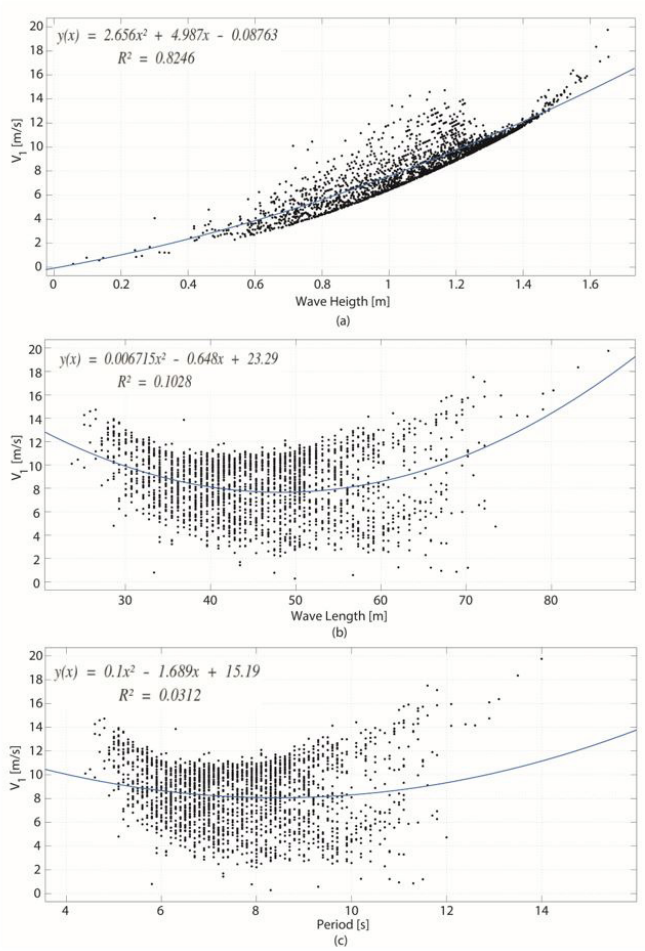

Figure 9. Correlations between air velocity in section 1 and wave height (a), wave length (b), and wave period (c) for the case with 4 m deep.

It is also possible to observe on Figure 10 a fast decay of powers between *17* and *16* m depth. This remark can be explained by the use of Equations 8 and 13, which were applied to reproduce the natural behavior of waves that tend to break parallel to the beach. To represent this effect, those equations force the influence of the bottom at a single wave, which induce the monochromatic wave to respond for a right angle between depth of the incident wave and the bathymetric line, making the first response in terms of refraction more abrupt. During the trajectory towards shallow waters, the bathymetric lines are parallel, which decreases the impact of the refraction on the wave height.

It can be noted that the highest value of resource (wave) power does not necessarily correspond to the highest value of mechanical power extracted by device. This fact might occur because the OWC device extracts mechanical power using only the vertical velocity generated by the wave. However, the wave energy can be dissipated by other directions. In other words, the wave power dissipated by horizontal velocity, wave break, interaction with the ocean floor, for example, can not be converted by the OWC device and it is wasted. An example of this fact can be observed on Figure 10, for the cases of *4* and *6* m of depth.

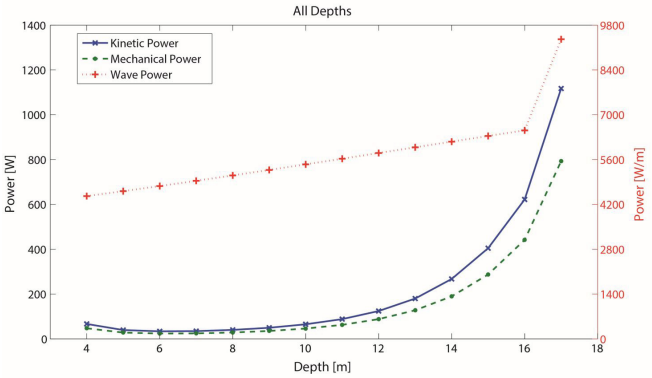

Figure 10. Powers variations in different depths.

Based on the model results it seems reasonable to use the proposed design of OWC attached to a previously built structure onshore to convert wave power. The performance would be better as long as the device is placed where the waves are less affected

by the bottom friction, since the wave length plays an important role in the kinetic and mechanical power.

The results shown in this paper present a more comprehensive view in comparison with the ones presented in Vecchia et al. (2015, 2016). These references use only the seasonal means of the wave parameters to perform the simulations and represent the preliminary studies of the proposed design of the OWC device. The use of time series on simulations and the procedures to estimate the wave parameters at different depths allow to evaluate the power extracted by the device at different conditions. These two aspects represent an important improvement to understand the roles of the wave parameters and its influence on the power extraction.

CONCLUSIONS

This paper presented an evaluation of a wave power extraction system installed near shore in a fishing pier at the coast of south Brazil. The simulation results of a mathematical model of an OWC device were analyzed in terms of wave, kinetic and mechanical power for two depths and different seasons. These preliminary results could promote small scale solutions with special design aiming to integration with previous built structures.

Regarding the influence of the depth on the extracted power, a strong influence of the wavelength on the air velocity inside the tube was found at *17* m water depth. On the other hand, the wave height was the main variable that affects the airflow and, consequently, the power for *4* m water depth. The wave length reduction with the depth resulted in a decrease of *47* % on the annual wave power and *88* % on the kinetic power inside the tube.

It was also observed the response of the system according to the seasonal mean wave characteristics. For *4* m water depth, the simulation results indicate a better performance of the OWC in the spring and winter. A different response was obtained for *17*m deep, with a greater wave power in the winter, while the highest value of extracted mechanical power occurs in spring. Thus, it was noted that the greater value of resource (wave) power does not necessarily corresponds to the greater value of mechanical power extracted for the device.

To sum up, this study showed that the water depth and the annual seasons can affect the performance of the device. The presented results can be used to determine the most efficient place to install the OWC. For the case study presented in this paper, the performance would be better as long as the device were placed in a position where the waves are less influenced by the bottom friction, but it still has the necessary increment of the wave height.

All the presented results can be influenced by the complexity of irregular waves behavior. This aspect is one of the greatest challenges for simulating OWC converters. Keeping that in mind, the use of time series represents an important advance to improve the precision of the obtained simulation results. Another consideration could be the application of a numerical method to reproduce in a more complex and realistic way the influence of refraction and shoaling caused by the bottom. These points might be suggestions for improving the mathematical model of the OWC device. The inclusion of the electrical power generator is the next challenge to enhance the model.

ACKNOWLEDGEMENTS

Leonardo C. Dalla Vecchia received PIBIC scholarships from CNPq (National Council for Scientific and Technological Development), Brazil. The authors would like to thank Professor Elírio Toldo Junior for the wave data measurements and Mr. Arnold van Rooijen from Deltares and University of Western Australia for his help in reviewing the text of this paper.

REFERENCES

ALVES, J. H. G. M.; RIBEIRO, E. O.; MATHESON, G. S. G.; LIMA, J. A. M.; RIBEIRO, C. E. P. Reconstituição do clima de ondas no sul-sudeste brasileiro entre 1997 e 2005. *Revista Brasileira de Geofísica*, v. 27, n. 3, p. 427-445, 2009. http://dx.doi.org/10.1590/S0102-261X2009000300010.

ARINAGA, R. A.; CHEUNG, K. F. Atlas of global wave energy from 10 years of reanalysis and hind cast data. *Renewable Energy*, v. 39, n. 1, p. 49-64, 2012. http://dx.doi.org/10.1016/j.renene.2011.06.039.

ASSIS, L.; BELUCO, A.; ALMEIDA, L. Avaliação e aproveitamento da energia das ondas oceânicas no litoral do rio grande do sul. *Revista Brasileira de Recursos Hídricos*, v. 18, n. 3, p. 21-29, 2013. http://dx.doi.org/10.21168/rbrh.v18n3.p21-29.

ASTARIZ, S.; IGLESIAS, G. The economics of wave energy: a review. *Renewable and Sustainable Energy Reviews*, v. 45, p. 397-408, 2015. http://dx.doi.org/10.1016/j.rser.2015.01.061.

BINGHAM, H. B.; DUCASSE, D.; NIELSEN, K.; READ, R. Hydrodynamic analysis of oscillating water column wave energy devices. *Journal of Ocean Engineering and Marine Energy*, v. 1, n. 4, p. 405-419, 2015. http://dx.doi.org/10.1007/s40722-015-0032-4.

BOUALI, B.; LARBI, S. Contribution to the geometry optimization of an oscillating water column wave energy converter. *Energy Procedia*, v. 36, p. 565-573, 2013. http://dx.doi.org/10.1016/j.egypro.2013.07.065.

BRENDMO, A.; FALNES, J.; LILLEBEKKEN, P. Linear modeling of oscillating water columns including viscous loss. *Oceanographic Literature Review*, v. 5, n. 44, p. 429, 1997.

CARBALLO, R.; SÁNCHEZ, M.; RAMOS, V.; CASTRO, A. A tool for combined WEC-site selection throughout a coastal region: Rias Baixas, NW Spain. *Applied Energy*, v. 135, n. 1, p. 11-19, 2014. http://dx.doi.org/10.1016/j.apenergy.2014.08.068.

CONTESTABILE, P.; VINCENZO, F.; DI LAURO, E.; VICINANZA, D. Full-scale prototype of an overtopping breakwater for wave energy conversion. *Coastal Engineering Proceedings*, v. 1, n. 35, p. 12, 2017. http://dx.doi.org/10.9753/icce.v35.structures.12.

CORNETT, A. M. A global wave energy resource assessment. In: INTERNATIONAL OFFSHORE AND POLAR ENGINEERING CONFERENCE, 18., 2008, Vancouver. *Proceedings*… California:

International Society of Offshore and Polar Engineers, 2008. p. 318-326.

COSTA, P. R.; GARCIA-ROSA, P. B.; ESTEFEN, S. F. Phase control strategy for a wave energy hyperbaric converter. *Ocean Engineering*, v. 37, n. 17, p. 1483-1490, 2010. http://dx.doi.org/10.1016/j.oceaneng.2010.07.007.

DEAN, R. G.; DALRYMPLE, R. A. *Water wave mechanics for engineers and scientists*. Singapore: World Scientific, 1991. http://dx.doi.org/10.1142/1232.

DELMONTE, N.; BARATER, D.; GIULIANI, F.; COVA, P.; BUTICCHI, G. Review of oscillating water column converters. *IEEE Transactions on Industry Applications*, v. 52, n. 2, p. 1698-1710, 2016.

DIAS, G. C.; SANTOS, S. M.; SANTOS, E. D.; ROCHA, L. A. O.; OLINTO, C. R. Análise teórica da influência de perfis sobre a potência de uma turbina Wells empregada em dispositivos de conversão de energia das ondas. *VETOR: Revista de Ciências Exatas e Engenharias*, v. 23, n. 1, p. 44-56, 2013.

ESTEFEN, S.; COSTA, P. R.; PINHEIRO, M. M.; RICARTE, E.; MENDES, A.; ESPERANÇA, P. T. Geração de energia elétrica pelas ondas do mar. In: SEMINÁRIO INTERNACIONAL DE ENERGIA DE ONDAS, 2006, Rio de Janeiro. *Anais*... Rio de Janeiro: COPPE-UFRJ, 2006. p. 1-6.

FALCÃO, A. F. Wave energy utilization: a review of the technologies. *Renewable & Sustainable Energy Reviews*, v. 14, n. 3, p. 899-918, 2010. http://dx.doi.org/10.1016/j.rser.2009.11.003.

FALCÃO, A. F.; HENRIQUES, J. C. Oscillating-water-column wave energy converters and air turbines: a review. *Renewable Energy*, v. 85, p. 1391-1424, 2016. http://dx.doi.org/10.1016/j.renene.2015.07.086.

FOX, R. W.; MCDONALD, A. T.; PRITCHARD, P. J. *Introduction to fluid mechanics*. New York: John Wiley & Sons, 1985.

GARCIA-ROSA, P. B.; CUNHA, J. P. V. S.; LIZARRALDE, F.; ESTEFEN, S. F.; MACHADO, I. R.; WATANABE, E. H. Wave-to-wire model and energy storage analysis of an ocean wave energy hyperbaric converter. *IEEE Journal of Oceanic Engineering*, v. 39, n. 2, p. 386-397, 2014. http://dx.doi.org/10.1109/JOE.2013.2260916.

HODGINS, D. O.; LEBLOND, P. H.; HUNTLEY, D. A. *Shallow-water wave calculations*. Ottawa: Fisheries and Oceans, 1985. p. 10-75.

KO, C.-H.; TSAI, C.-P.; CHUANG, C.-Y.; CHEN, Y.-C. An experimental study of hydrodynamics of an improved owc converter. In: INTERNATIONAL OCEAN AND POLAR ENGINEERING CONFERENCE, 27., 2017, São Francisco. *Proceedings*… California: International Society of Offshore and Polar Engineers, 2017.

LIANG, C.; ZUO, L. On the dynamics and design of a two-body wave energy converter. *Renewable Energy*, v. 101, p. 265-274, 2017. http://dx.doi.org/10.1016/j.renene.2016.08.059.

MISHRA, S. K.; PURWAR, S.; KISHOR, N. An optimal and non-linear speed control of oscillating water column wave energy plant with wells turbine and DFIG. *International Journal of Renewable Energy Research*, v. 6, n. 3, 2016.

MOHAMED, M. H. A. *Design optimization of Savonius and Wells turbines*. Magdeburg: Otto-von-Guericke University Magdeburg, 2011.

NATY, S.; VIVIANO, A.; FOTI, E. Wave energy exploitation system integrated in the coastal structure of a mediterranean port. Sustainability. *Multidisciplinary Digital Publishing Institute*, v. 8, n. 12, p. 1342, 2016.

PIANCA, C.; MAZZINI, P. L. F.; SIEGLE, E. Brazilian offshore wave climate based on nww3 reanalysis. *Brazilian Journal of Oceanography*, v. 58, n. 1, p. 53-70, 2010. http://dx.doi.org/10.1590/S1679-87592010000100006.

RAGHUNATHAN, S.; TAN, C. P.; OMBAKA, O. O. Performance of the Wells self-rectifying air turbine. *Journal of the Royal Aeronautical Society*, v. 89, n. 890, p. 369-379, 1985.

REZANEJAD, K.; GUEDES SOARES, C.; LÓPEZ, I.; CARBALLO, R. Experimental and numerical investigation of the hydrodynamic performance of an oscillating water column wave energy converter. *Renewable Energy*, v. 106, p. 1-16, 2017. http://dx.doi.org/10.1016/j.renene.2017.01.003.

SIEGLE, E.; ASP, N. E. Wave refraction and longshore transport patterns along the southern Santa Catarina coast. *Brazilian Journal of Oceanography*, v. 55, n. 2, p. 109-120, 2007. http://dx.doi.org/10.1590/S1679-87592007000200004.

STRAUCH, J.; CUCHIARA, D.; TOLDO JUNIOR, E. E.; ALMEIDA, L. E. S. B. O padrão das ondas de verão e outono no litoral sul e norte do rio grande do sul. *Revista Brasileira de Recursos Hídricos*, v. 14, n. 4, p. 29-37, 2009. http://dx.doi.org/10.21168/rbrh.v14n4.p29-37.

TESSLER, M. G.; GOYA, S. C. Processos costeiros condicionantes do litoral brasileiro. *Revista do Departamento de Geografia*, v. 17, n. 8, p. 11-23, 2005.

TOLDO, E. E.; ALMEIDA, L. E. S. B.; NICOLODI, J. L.; ABSALONSEN, L.; GRUBER, N. L. S. O controle da deriva litorânea no desenvolvimento do campo de dunas e da antepraia no litoral médio do rio grande do sul. *Pesquisas em Geociências*, v. 33, n. 2, p. 35-42, 2006.

VECCHIA, L. C. D.; FARIAS, C. F.; SCHARLAU, C. C.; D'AQUINO, C. A. Modelagem e dimensionamento de um sistema de geração de energia a partir das ondas do oceano. In: CONGRESSO BRASILEIRO DE AUTOMÁTICA, 21., 2016, Vitória . *Anais*... Campinas: SBA, 2016. p. 750-755.

VECCHIA, L. C. D.; SCHARLAU, C. C.; D'AQUINO, C. A.; ANTUNES, V.; PFITSCHER, L. L. Modeling of wave energy absorption: a case study for a fishing pier in brazil. In: INTERNATIONAL UNIVERSITIES POWER ENGINEERING CONFERENCE (UPEC), 50., 2015, Stoke-on-Trent, UK. *Proceedings*… USA: IEEE, 2015. p. 1-6. http://dx.doi.org/10.1109/UPEC.2015.7339969.

VEIGAS, M.; LOPEZ, M.; ROMILLO, P.; CARBALLO, R.; CASTRO, A.; IGLESIAS, G. A proposed wave farm on the galician coast. *Energy Conversion and Management*, v. 99, p. 102-111, 2015. http://dx.doi.org/10.1016/j.enconman.2015.04.033.

WEBSTER, M.; GATO, L. M. C. The effect of rotor blade shape on the performance of the Wells turbine. In: INTERNATIONAL OFFSHORE AND POLAR ENGINEERING CONFERENCE, 9., 1999, Brest, France. *Proceedings*… California: International Society of Offshore and Polar Engineers, 1999. p. 169-173.

WRIGHT, L.; SHORT, A. D. Morphodynamic variability of surf zones and beaches: a synthesis. *Marine Geology*, v. 56, n. 1, p. 93-118, 1984. http://dx.doi.org/10.1016/0025-3227(84)90008-2.

Authors contributions

Carla de Abreu D'Aquino: Wave data analysis, input wave data organization, small scale device conception using previously built structures.

Cesar Cataldo Scharlau: Device mathematical modeling, output power evaluation, small scale device conception using previously built structures.

Leonardo Casagrande Dalla Vecchia: Wave and fluid mechanic data preparation for simulations, device mathematical modeling, model developed and programming using Matlab.